Published in final edited form as:
ACS Catal. 2013 August 2; 3(8): 1685–1692. doi:10.1021/cs400332y.

Photocatalytic Conversion of CO_2 to CO using Rhenium Bipyridine Platforms Containing Ancillary Phenyl or BODIPY Moieties

Gabriel A. Andrade[§], **Allen J. Pistner**[§], **Glenn P.A. Yap**[§], **Daniel A. Lutterman**[*,†], and **Joel Rosenthal**[*,§]

[§]Department of Chemistry and Biochemistry, University of Delaware, Newark, DE, 19716

[†]Chemical Sciences Division Oak Ridge National Laboratory, Oak Ridge, TN, 37831

Abstract

Harnessing of solar energy to drive the reduction of carbon dioxide to fuels requires the development of efficient catalysts that absorb sunlight. In this work, we detail the synthesis, electrochemistry and photophysical properties of a set of homologous *fac*-$Re^{I}(CO)_3$ complexes containing either an ancillary phenyl (**8**) or BODIPY (**12**) substituent. These studies demonstrate that both the electronic properties of the rhenium center and BODIPY chromophore are maintained for these complexes. Photolysis studies demonstrate that both assemblies **8** and **12** are competent catalysts for the photochemical reduction of CO_2 to CO in DMF using triethanolamine (TEOA) as a sacrificial reductant. Both compounds **8** and **12** display TOFs for photocatalytic CO production upon irradiation with light ($\lambda_{ex} \geq 400$ nm) of ~5 hr^{-1} with TON values of approximately 20. Although structural and photophysical measurements demonstrate that electronic coupling between the BODIPY and *fac*-$Re^{I}(CO)_3$ units is limited for complex **12**, this work clearly shows that the photoactive BODIPY moiety is tolerated during catalysis and does not interfere with the observed photochemistry. When taken together, these results provide a clear roadmap for the development of advanced rhenium bipyridine complexes bearing ancillary BODIPY groups for the efficient photocatalytic reduction of CO_2 using visible light.

Keywords

BODIPY; carbon dioxide; catalysis; electrochemistry; photochemistry; rhenium bipyridine derivatives

Introduction

The reduction of carbon dioxide is a promising strategy for energy storage via the sustainable production of fuels.[1,2] To this end, the development of efficient methods and platforms for conversion of CO_2 to CO may enable the production of synthetic petroleum using existing Fisher-Tropsch chemistry.[3–5] Photocatalytic reduction of CO_2 is especially attractive in this regard, as this approach allows for the direct conversion of sunlight to energy-rich commodity chemicals.[6,7] As such, the development of new molecular photocatalysts for CO_2 reduction is an active and important area of research.[8]

[*]**Corresponding Author**. luttermanda@ornl.gov, joelr@udel.edu.

ASSOCIATED CONTENT

Supporting Information Spectroscopic and crystallography data. This material is available free of charge via the Internet at http://pubs.acs.org.

Transition metal complexes have been repeatedly targeted as catalysts for CO_2 activation and photoreduction.[9] Properly designed systems of this type are attractive as they can support the multielectron redox chemistry necessary to drive the uphill conversion of CO_2 to reduced carbon-containing products. Of the many platforms developed for the photochemical activation of carbon dioxide,[10–15] *fac*-$Re^{I}(CO)_3$ derivatives supported by bipyridine ligands have shown excellent efficiencies for the reduction of CO_2 to CO.[16–26] As initially demonstrated by Lehn and coworkers, excitation of the metal-to-ligand charge transfer (MLCT) transition of platforms such as $Re(bpy)(CO)_3Cl$ in the presence of a sacrificial reductant such as triethanol amine (TEOA) leads to formation of a reduced rhenium complex that efficiently drives conversion of CO_2 to CO.[27] A major limitation of these traditional Re complexes, however, is their lack of significant absorption features in the visible region. The inability of these systems to harvest solar energy at wavelengths longer than ~430 nm is a critical impediment to the use of sunlight to drive CO_2 reduction, since the solar power spectrum is most intense from approximately 425 – 600 nm.[28]

To confront the truncated absorption spectra of $Re(bpy)(CO)_3Cl$ derivatives, analogous platforms with broadened MLCT transitions[29] or containing pendant visible light absorbing complexes have been studied.[30,31] This later strategy has proven to be particularly promising, as *fac*-$Re^{I}(CO)_3$ complexes covalently tethered to metalloporphyrins[32–34] can photocatalyze the reduction of CO_2 to CO using longer wavelength light.[35] Building on this work, we rationalized that tethering of an organic chromophore to a $Re(bpy)(CO)_3Cl$ construct might lead to a similar photocatalysis while avoiding the need for arduous porphyrin syntheses and purification steps. In choosing an organic chromophore, we turned to the BODIPY class of dye, as these indacene frameworks are easily prepared and absorb strongly in the visible region in a manner, which complements the typical absorption profile of $Re(bpy)(CO)_3Cl$ complexes. Moreover, since pyrromethene dyes can serve as photoreductants,[36] we rationalized that excitation of a BODIPY chromophore linked to a $Re(bpy)(CO)_3Cl$ unit would facilitate formation of $Re(bpy^{\bullet-})(CO)_3Cl$ and drive CO_2 catalysis via a photoinduced electron transfer (PET) pathway.

Based on this rationale, we have developed a modular synthetic strategy that allowed for a robust BODIPY dye to be tethered to a *fac*-$Re^{I}(CO)_3$ moeity via a triazole linker. In this study, we detail the redox properties of this BODIPY appended rhenium complex and demonstrate that this assembly supports a photocatalysis with CO_2. Moreover, we show that the topology of the bridge connecting the $Re(bpy)(CO)_3Cl$ and BODIPY units is an important consideration in designing assemblies for the photochemical reduction of CO_2.

Experimental Section

General Materials and Methods

Reactions were performed in oven-dried round-bottomed flasks unless otherwise noted. Reactions that required an inert atmosphere were conducted under a positive pressure of N_2 using flasks fitted with Suba-Seal rubber septa or in a nitrogen filled glove box. Air and moisture sensitive reagents were transferred using standard syringe or cannula techniques. Reagents and solvents were purchased from Sigma Aldrich, Acros, Fisher, Strem, or Cambridge Isotopes Laboratories. Solvents for synthesis were of reagent grade or better and were dried by passage through activated alumina and then stored over 4 Å molecular sieves prior to use.[37] Column chromatography was preformed with 40–63 μm silica gel with the eluent reported in parentheses. Analytical thin-layer chromatography (TLC) was performed on precoated glass plates and visualized by UV or by staining with $KMnO_4$. 4-Hydroxymethyl-4'-methyl-2,2'-bipyridine (**2**),[38] 4-Bromomethyl-4'-methyl-2,2'-bipyridine (**3**),[38] and BODIPY derivatives (**9** and **10**)[39] were prepared as previously described in literature.

Compound Characterization

^{1}H NMR and ^{13}C NMR spectra were recorded at 25 °C on a Bruker 400 MHz spectrometer. Proton spectra are referenced to the residual proton resonance of the deuterated solvent ($CDCl_3$ = δ 7.26; CD_3CN = δ 1.94; $(CD_3)_2SO$ = δ 2.50) and carbon spectra are referenced to the carbon resonances of the solvent ($CDCl_3$ = δ 77.16; CD_3CN = δ 1.32, 118.26; $(CD_3)_2SO$ = δ 39.52). All chemical shifts are reported using the standard δ notation in parts-per-million; positive chemical shifts are to higher frequency from the given reference. LR-GCMS data were obtained using an Agilent gas chromatograph consisting of a 6850 Series GC System equipped with a 5973 Network Mass Selective Detector. Low resolution MS data was obtained using either a LCQ Advantage from Thermofinnigan or a Shimadzu LC/MS-2020 single quadrupole MS coupled with an HPLC system, with dual ESI/APCI source. High-resolution mass spectrometry analyses were either performed by the Mass Spectrometry Laboratory in the Department of Chemistry and Biochemistry at the University of Delaware or at the University of Illinois at Urbana-Champaign. Infra-red spectra were recorded in KBr using a Nicolet Magna-IR 750 spectrometer.

Electrochemical Measurements

All electrochemistry was performed using either a CHI-620D potentiostat/galvanostat or a CHI-760D bipotentiostat. Cyclic voltammetry was performed using a standard three-electrode configuration. CV scans were recorded for quiescent solutions using a glassy carbon working disk electrode (3.0 mm diameter CH Instruments) and a platinum wire auxiliary electrode. All potentials were measured against a silver wire pseudo reference with a ferrocene internal standard and were adjusted to the saturate calomel electrode (SCE) via the relation Fc/Fc^{+} = 460 mV + SCE. CV experiments were performed in DMF using 0.1 M tetrabutylammonium hexafluorophosphate ($TBAPF_6$) as the supporting electrolyte. Concentrations of analytes were 1 mM.

UV-vis Absorption Experiments

UV/visible absorbance spectra were acquired on a StellarNet CCD array or Agilent 8453 Diode Array UV-vis spectrometer using screw cap quartz cuvettes (6q or 7q) of 1 cm pathlength from Starna. All absorbance spectra were recorded at room temperature. All samples for spectroscopic analysis were prepared in DMF.

Steady-State Fluorescence Measurements

Spectra were recorded on an automated Photon Technology International (PTI) QuantaMaster 40 fluorometer equipped with a 75-W Xenon arc lamp, a LPS-220B lamp power supply and a Hamamatsu R2658 photomultiplier tube. Samples for fluorescence analysis were prepared in an analogous method to that described above for the preparation of samples for UV-vis spectroscopy. Samples were excited at λ_{ex} = 500 nm and emission was monitored from 510–800 nm with a step size of 1 nm and integration time of 0.5 seconds. Reported spectra are the average of at least three individual acquisitions.

Emission quantum yields were calculated using $[Ru(phen)_3]Cl_2$ (phen = 1,10-phenanthroline) in water (Φ_{ref} = 0.072)[40,41] as the reference actinometer using the expression below,[42]

$$\Phi_{em}=\Phi_{ref}\left(\frac{A_{ref}}{A_{em}}\right)\left(\frac{I_{em}}{I_{ref}}\right)\left(\frac{\eta_{em}}{\eta_{ref}}\right)^2$$

where Φ_{em} and Φ_{ref} are the emission quantum yield of the sample and the reference, respectively, A_{ref} and A_{em} are the measured absorbance of the reference and sample at the excitation wavelength, respectively, I_{ref} and I_{em} are the integrated emission intensities of the reference and sample, respectively, and η_{ref} and η_{em} are the refractive indices of the solvents of the reference and sample, respectively.

Time-Resolved Fluorescence Measurements

Time correlated single photon counting (TCSPC) experiments were performed on an IBH (Jobin Yvon Horiba) model 5000F instrument equipped with single monochromators on both the excitation and emission sides of the instrument. The excitation light source was a NanoLED with a short 1.3 ns pulse width at 458 nm. Emission signals were collected on a picosecond photon detection module (TBX-04) at an angle perpendicular to excitation for samples and blanks. Data was collected at the sample's peak maxima as determined by steady state experiments described above to obtain the decay profile. Decay analysis and curve fitting routines to determine the sample's lifetimes were performed by the software (DAS6) provided by the manufacturer (IBH).

X-ray Structure Determination

Crystals were mounted using viscous oil onto a plastic mesh and cooled to the data collection temperature. Data were collected on a Bruker-AXS APEX 2 DUO CCD diffractometer with Mo-Kα radiation (λ=0.71073 Å) monochromated with graphite. Unit cell parameters were obtained from 60 data frames, 0.5° ω, from three different sections of the Ewald sphere. The systematic absences in the diffraction data are uniquely consistent with $P2_1/n$. The data-set was treated with multi-scan absorption corrections (Apex2 software suite, Madison, WI, 2005). The structure was solved using direct methods and refined with full-matrix, least-squares procedures on F^2.[43] All non-hydrogen atoms were refined with anisotropic displacement parameters. The amide H-atom was located from the electron density difference Fourier map and refined with the isotropic parameter constrained to be equal to 1.2 of the equivalent isotropic parameter of the attached N-atom. All other hydrogen atoms were treated as idealized contributions. Atomic scattering factors are contained in the SHELXTL 6.12 program library. The CIF has been deposited under CCDC 936531.

Photocatalytic CO_2 Reduction and Headspace Analysis

Samples (1.5 mM) of **8** and **12** were prepared in 5:1 DMF:triethanol amine to a total volume of 3 mL in a 8 mL cuvette. The samples were charged with a stir bar and the system was sealed with a rubber septum which was tightened with a copper wire. The sample solution and cuvette headspace was saturated with CO_2 by sparging for 25 minutes. The samples were irradiated with light from a 200 W Xe arc lamp (Oriel Instruments Model 66057). The wavelength of light was controlled by passing it through a long pass filter (λ > 400 or 495 nm) that was immersed in water. Light was focused onto the stirred sample and irradiated for 4.5 or 17 hrs. After irradiation, aliquots were analyzed by gas chromatography coupled to a methanizer and flame ionization detector (GC-FID) for CO production and a known quantity of CO was injected for normalization purposes.

[Re(4-Bromomethyl-4'-methyl-2,2'-bipyridine)$(CO)_3$Cl] (4)

This compound was prepared using a slightly modified literature procedure.[44] 4-Bromomethyl-4'-methyl-2,2'-bipyridine (0.526 g, 2.0 mmol) and $Re(CO)_5Cl$ (0.723 g, 2.0 mmol) were dissolved in 100 ml of toluene. The reaction mixture was heated at reflux under air with stirring. After 12 hrs, the reaction was allowed to cool to room temperature and the resulting yellow solid that precipitated from solution was collected by filtration and washed

with hexanes The crude yellow material was combined with tetrabutylammonium chloride (0.066g, 0.239 mmol) in 25 ml of MeCN and stirred under air at room temperature. After 12 hrs this solution was filtered through a plug of celite and the filtrate was concentrated under reduced pressure. The resultant material was purified via flash column chromatography on silica using CH_2Cl_2 as the eluent to deliver 0.994g of the title compound in 87 % yield. ^{1}H NMR (400 MHz, DMSO, 25 °C) δ/ppm: 9.03 (d, J = 5.7 Hz, 1H), 8.87 (d, J = 5.6 Hz, 1H), 8.82 (s, 1H), 8.67 (s, 1H), 7.79 (d, J = 5.7 Hz, 1H), 7.60 (d, J = 5.7 Hz, 1H), 4.99 (s, 2H), 2.57 (s, 3H).^{13}C NMR (101 MHz, DMSO, 25 °C) δ/ppm: 197.41, 197.30, 189.57, 155.77, 154.48, 153.53, 152.55, 152.46, 150.58, 128.71, 127.07, 125.17, 123.66, 43.41, 20.97. HR-LIFDI-MS $[M]^+$ *m/z*: calc for $C_{15}H_{11}BrClN_2O_3Re$, 567.9177; found, 567.9202. ν_{max} (KBr)/cm^{-1} 2026, 1897, 1871 (s, CO).

[Re(4-Azidomethyl-4'-methyl-2,2'-bipyridine)(CO)$_3$Cl] (5)

This compound was prepared using a slightly modified literature procedure.[45] Sodium azide (9.4 mg, 0.15 mmol) was dissolved in 3 ml of DMSO and stirred at room temperature for 12 hrs. This solution was added to 75 mg (0.13 mmol) of [Re(4-Bromomethyl-4'-methyl-2,2'-bipyridine)(CO)$_3$Cl] (**4**) and the resulting mixture was stirred at room temperature for 2 hrs. Water (10 ml) was then added to the reaction and this mixture was allowed to stir for 20 min. The mixture was then extracted three times with CH_2Cl_2 and the organic extract was then washed twice with distilled water (20 ml) and once with brine (20 ml). The organic layer was separated, dried over Na_2SO_4 and the solvent was removed under reduced pressure to yield 65 mg (93%) of the desired product as a dark yellow powder. ^{1}H NMR (400 MHz, DMSO, 25 °C) δ/ppm: 9.00 (d, J = 5.7 Hz, 1H), 8.86 (d, J = 5.7 Hz, 1H), 8.70 (s, 2H), 7.70 (d, J = 5.6 Hz, 1H), 7.60 (d, J = 5.5 Hz, 1H), 4.88 (s, 2H), 2.57 (s, 3H). ^{13}C NMR (101 MHz, DMSO, 25 °C) δ/ppm: 197.44, 197.37, 189.63, 155.61, 154.59, 153.25, 152.52, 152.45, 150.03, 128.65, 126.10, 125.19, 122.63, 51.94, 20.96. HR-LIFDI-MS $[M]^+$ *m/z*: calc for $C_{15}H_{11}ClN_5O_3Re$, 531.0099; found, 531.0076. ν_{max} (KBr)/cm^{-1} 2021, 1910, 1886 (s, CO) 2113 (s, N_3).

N-(benzoyloxy)succinimide (6)

DCC (2.68 g, 13.0 mmol) and *N*-hydroxysuccinimide (1.49 g, 13.0 mmol) were added to a solution of benzoic acid (1.24 g, 10.0 mmol) dissolved in 100 mL of THF. The reaction solution was stirred at room temperature for 20 hrs, following which, the mixture was filtered. The filtrate was concentrated under reduced pressure and the resulting residue was purified via flash column chromatography on silica using CH_2Cl_2 and CH_3OH (97:3) as the eluent to deliver 2.17 g (92%) of the title compound as a pale yellow solid. ^{1}H NMR (400 MHz, $CDCl_3$, 25 °C) δ/ppm: 8.18 – 8.12 (m, 2H), 7.69 (t, *J* = 7.5 Hz, 1H), 7.52 (t, *J* = 7.8 Hz, 2H), 2.92 (s, 4H). ^{13}C NMR (101 MHz, $CDCl_3$, 25 °C) δ/ppm: 169.46, 162.07, 135.16, 130.81, 129.07, 125.31, 77.23, 25.89. HR-CI-MS $[M+H]^+$ *m/z*: calc for $C_{11}H_{10}NO_4$, 220.0610; found, 220.0622.

N-propargylbenzamide (7)

Compoud **6** (100 mg, 0.425 mmol) was dissolved in 10 mL of CH_2Cl_2 and degassed with N_2 for 5 min. Propargylamine (55 μL, 0.85 mmol) and triethylamine (590 μL, 4.25 mmol) were added and the reaction was stirred at room temperature for 18 hrs under an atmosphere of N_2. The reaction was then washed twice with water and dried over Na_2SO_4. The solvent was removed under reduced pressure and the resulting residue was purified via flash column chromatography on silica using CH_2Cl_2 and CH_3OH (95:5) as the eluent to deliver 62 mg (92%) of the title compound as a white solid. ^{1}H NMR (400 MHz, $CDCl_3$, 25 °C) δ/ppm: 7.83 – 7.76 (m, 2H), 7.56 – 7.49 (m, 1H), 7.49 – 7.41 (m, 2H), 6.33 (s, 1H), 4.26 (dd, *J* = 5.2, 2.6 Hz, 2H), 2.29 (t, *J* = 2.6 Hz, 1H). ^{13}C NMR (101 MHz, $CDCl_3$, 25 °C) δ/ppm:

167.29, 133.90, 132.04, 128.86, 127.20, 79.63, 72.16, 30.01. HR-EI-MS $[M]^+$ *m/z*: calc for $C_{10}H_9NO$, 159.0684; found, 159.0689.

[Re(Mebpy)(CO)$_3$Cl]–Phenyl (8)

Complex **5** (100 mg, 190 μmol), propargylamide **7** (45 mg, 280 μmol), $CuSO_4$ (5.0 mg, 19 μmol) and ascorbic acid (5.0 mg, 30 μmol) were combined in an oven dried Schlenk flask that was cooled under vacuum. The reactants were dissolved in 6 mL of anhydrous DMF and the reaction was stirred at room temperature under N_2 for 18 hrs. CH_2Cl_2 (10 mL) was added to the reaction and the solution was washed three times with brine and dried over Na_2SO_4. The solvent was removed under reduced pressure and the resulting residue was purified via flash column chromatography on silica using CH_2Cl_2 and CH_3OH (95:5) as the eluent to deliver 97 mg (74%) of the title compound as an orange solid. ^{1}H NMR (400 MHz, CD_3CN, 25 °C) δ/ppm: 8.95 (d, J = 5.8 Hz, 1H), 8.84 (d, J = 5.7 Hz, 1H), 8.20 (d, J = 8.9 Hz, 2H), 7.91 (s, 1H), 7.79 (d, J = 5.3, 2H), 7.60 – 7.49 (m, 2H), 7.48 – 7.40 (m, 3H), 7.34 (dd, J = 5.7, 1.7 Hz, 1H), 5.75 (s, 2H), 4.64 (d, J = 5.8 Hz, 2H), 2.53 (s, 3H). ^{13}C NMR (101 MHz, CD_3CN, 25 °C) δ/ppm: 198.36, 198.27, 190.15, 167.78, 157.19, 155.65, 154.33, 153.58, 153.40, 149.96, 135.29, 132.34, 129.38, 129.34, 127.93, 126.55, 125.84, 124.59, 123.22, 52.68, 35.97, 21.44. HR-ESI-MS $[M\text{-}Cl]^+$ *m/z*: calc for $C_{25}H_{20}N_6O_4Re$, 655.1104; found, 655.1117. ν_{max} (KBr)/cm^{-1} 2024, 1929, 1885 (s, CO).

8-(4-(N-(prop-2-yn-1-yl)benzamide)-2,8-diethyl-1,3,7,9-tetramethyl-BODIPY (11)

BODIPY derivative **10** (100 mg, 0.19 mmol) was dissolved in 20 mL of CH_2Cl_2 and the resulting solution was sparged with N_2 for 5 minutes. Propargylamine (26 μL, 0.38 mmol) and triethylamine (264 μL, 1.9 mmol) were added to the solution and the reaction was stirred at room temperature for 18 hrs under an atmosphere of N_2. The reaction was washed twice with water, dried over Na_2SO_4 and the solvent was then removed under reduced pressure. The reaction was purified via flash column chromatography on silica using CH_2Cl_2 and CH_3OH (50:1) as the eluent to deliver 74 mg (84%) of the title compound as a red solid. ^{1}H NMR (400 MHz, $CDCl_3$, 25 °C) δ/ppm: 7.93 (d, *J* = 8.2 Hz, 2H), 7.41 (d, *J* = 8.2 Hz, 2H), 6.37 (s, 1H), 4.32 (dd, *J* = 5.1, 2.6 Hz, 2H), 2.53 (s, 6H), 2.33 (t, J = 2.67Hz, 1H), 2.29 (q, *J* = 7.6 Hz, 4H), 1.25 (s, 6H), 0.98 (t, *J* = 7.5 Hz, 6H). ^{13}C NMR (101 MHz, $CDCl_3$, 25 °C) δ/ppm: 166.49, 154.42, 139.68, 138.73, 138.27, 134.15, 133.28, 130.49, 128.97, 128.03, 79.48, 72.17, 30.06, 17.21, 14.78, 12.74, 12.04. HR-EI-MS $[M]^+$ *m/z*: calc for $C_{27}H_{30}BN_3OF_2$, 461.2450; found, 461.2459. ν_{max} (KBr)/cm^{-1} 2021, 1914, 1897 (s, CO).

[Re(Mebpy)(CO)$_3$Cl]–BODIPY (12)

Rhenium complex **5** (40 mg, 75 μmol), BODIPY-Propargylamide **8** (42 mg, 90 μmol), $CuSO_4$ (2 mg, 7.5 μmol) and ascorbic acid (2 mg, 11 μmol) were combined in a Schlenk flask that was oven dried and cooled under vacuum. The flask was evacuated and backfilled with N_2 three times and the reactants were then dissolved in 4 mL of anhydrous DMF. The reaction mixture was stirred at room temperature for 15 hrs under an atmosphere of N_2, after which time, 10 mL of CH_2Cl_2 was added. The resulting solution was washed twice with brine and dried over Na_2SO_4. After removing the solvent under reduced pressure, the resultant material was purified via flash column chromatography on silica using CH_2Cl_2 and CH_3OH (9:1) as the eluent to deliver 50 mg (67%) of the title compound as a red solid. ^{1}H NMR (400 MHz, CD_3CN, 25 °C) δ/ppm: 8.95 (d, *J* = 5.8 Hz, 1H), 8.83 (d, *J* = 5.7 Hz, 1H), 8.23 (d, *J* = 1.9 Hz, 2H), 7.98 – 7.91 (m, 4H), 7.77 (t, *J* = 5.8 Hz, 1H), 7.46 – 7.38 (m, 3H), 7.35 (dd, *J* = 5.9, 1.7 Hz, 1H), 5.76 (s, 2H), 4.67 (d, *J* = 5.7 Hz, 2H), 2.53 (s, 3H), 2.46 (s, 6H), 2.30 (q, *J* = 7.5 Hz, 4H), 1.24 (s, 6H), 0.94 (t, *J* = 7.5 Hz, 6H). ^{13}C NMR (101 MHz, CD_3CN, 25 °C) δ/ppm: 198.32, 198.23, 190.12, 167.20, 157.19, 155.62, 154.82, 154.32, 153.55, 153.39, 149.89, 146.85, 140.60, 139.53, 139.33, 135.75, 134.10, 131.07, 129.51,

129.34, 128.84, 126.57, 125.85, 124.72, 123.27, 52.70, 36.02, 21.49, 17.42, 14.82, 12.72, 12.09. HR-ESI-MS $[M\text{-}Cl]^+$ *m/z*: calc for $C_{42}H_{41}BF_2N_8O_4Re$, 957.2870; found, 957.2879.

8-(4-(benzamido)methyl-1-benzyl-1H-1,2,3-triazole)-2,8-diethyl-1,3,7,9-tetramethyl-BODIPY (13)

BODIPY derivative **11** (33 mg, 72 μmol), benzyl azide (11 mg, 86 μmol), ascorbic acid (2 mg, 11 μmol), and $CuSO_4$ (2 mg, 7 μmol) were placed in a Schlenk flask under an atmosphere of N_2. The reactants were dissolved in anhydrous DMF (6 ml) and the resulting mixture was stirred at room temperature under N_2 for 12 hrs. CH_2Cl_2 (15 mL) was added to the reaction and the resulting solution was washed three times with brine and dried over Na_2SO_4. The solvent was removed under reduced pressure and the resulting residue was dissolved in 1 mL of CH_2Cl_2. The product was precipitated from the CH_2Cl_2 solution with diethyl ether (12ml), collected via filtration and washed with an additional 12 ml of diethyl ether to yield 37 mg (86%) of the title compound as a dark red powder. ^{1}H NMR (400 MHz, DMSO, 25 °C) δ/ppm: 9.22 (t, J = 5.7 Hz, 1H), 8.10 (s, 1H), 8.05 (d, J = 8.3 Hz, 2H), 7.48 (d, J = 8.3 Hz, 2H), 7.41 – 7.30 (m, 5H), 5.58 (s, 2H), 4.53 (d, J = 5.6 Hz, 2H), 2.44 (s, 6H), 2.28 (q, J = 7.4 Hz, 4H), 1.23 (s, 6H), 0.93 (t, J = 7.5 Hz, 6H). ^{13}C NMR (101 MHz, DMSO, 25 °C) δ/ppm: 165.44, 153.52, 145.14, 139.66, 138.05, 137.71, 136.22, 134.50, 132.79, 129.70, 128.79, 128.31, 128.21, 128.16, 128.07, 123.33, 52.74, 34.96, 16.44, 14.58, 12.32, 11.53. HR-LIFDI-MS $[M]^+$ *m/z*: calc for $C_{34}H_{37}BF_2N_6O$, 594.3096; found, 594.3076.

Results and Discussion

The synthesis of the azide appended rhenium bipyridine complex (**5**) is shown in Scheme 1. This pathway began with conversion of commercially available 4,4′-Dimethyl-2,2′-bipyridine (**1**) to the corresponding mono-alchohol via oxidation of a methyl group using SeO_2 followed by reduction to the alcohol using $NaBH_4$ to yield 4-hydroxymethyl-4’-methyl-2,2’-bipyridine (**2**). Treatment of compound **2** with HBr/H_2SO_4 delivered 4-bromomethyl-4’-methyl-2,2’-bipyridine (**3**),[38] which was then metallated with $Re(CO)_5Cl$ in refluxing toluene to deliver the corresponding bromomethyl-rhenium bipyridine complex (**4**). Substitution of the bromide for azide was accomplished using NaN_3 in DMSO to deliver the desired rhenium synthon (**5**) in excellent yield. With this complex in hand, the phenyl appended rhenium derivative (**8**) was prepared via standard Huisgen coupling with N-propargylbenzamide (**7**) using $CuSO_4$ and ascorbic acid in DMF. This reaction afforded the phenyl-amide appended $Re(bpy)(CO)_3Cl$ complex in nearly 75% yield.

The BODIPY tagged rhenium complex was prepared using an analogous strategy, as shown in Scheme 2. BODIPY carboxylic acid derivative **9**, the synthesis of which has been described previously,[39] was converted to the corresponding *N*-hydroxysuccinimide ester (**10**) via a standard EDC coupling. Compound **10** was subsequently treated with propargylamine in the presence of triethylamine to deliver the BODIPY-propargylamide (**11**). With the terminal alkyne functionality in place, the BODIPY unit was tethered to the azide functionalized rhenium complex (**5**) described above using a Huisgen coupling reaction similar to that employed for the preparation of complex **8**. This method allowed for the isolation of the desired BODIPY-amide appended $Re(bpy)(CO)_3Cl$ complex (**12**) in nearly 70% yield following purification. Alkyne **11** also allowed for preparation of a BODIPY photocontrol compound via Huisgen coupling with benzylazide to deliver **13**.

Prior to studying the ability of **8** and **12** to photochemically activate CO_2, the redox properties of these rhenium complexes were ascertained via cyclic voltammetry. Polarization curves recorded for 1.0 mM solutions of **8** (red) and **12** (blue) in DMF containing 0.1 M $TBAPF_6$ under an atmosphere of N_2 is shown in Figure 1. The CV

recorded for the phenyl appended complex (**8**) is similar to that observed for other simple $Re(bpy)(CO)_3Cl$ complexes,[44] exhibiting a reversible single electron reduction at −1.39 V versus SCE, which can be attributed to reduction of the bipyridine ligand and an irreversible $Re^{I/0}$ couple centered at approximately −1.88 V. The BODIPY-appended rhenium complex (**12**) supports a slightly more complex redox chemistry with four apparent reduction waves. Two of these waves are nearly superimposable with the bipyridine and metal centered reductions observed for control complex **8** and are believed to correspond to the analogous processes for the BODIPY-rhenium construct. The additional two waves, which are centered at approximately −1.15 and −1.98 V versus SCE are consistent with the first and second one electron reduction of the BODIPY moiety.[46–48] This assignment was confirmed by recording the CV trace for BODIPY control compound **13** (orange dashed), which is also presented in Figure 1.

The electrochemistry of complexes **8** and **12** was also probed in the presence of CO_2. As shown in Figures 2a and 2b, the CV profiles obtained for the phenyl and BODIPY appended rhenium complexes in DMF under an atmosphere of CO_2 is significantly altered compared to the corresponding trace recorded under N_2. The ligand reduction waves are largely unchanged in the presence of CO_2, however, a notable increase in current is observed upon scanning to potentials more negative than approximately −1.75 V (Figure 2). This observation is consistent with the electrocatalytic activation of CO_2 upon reduction of the Re^I centers of complexes **8** and **12**. This mechanistic pathway for CO_2 reduction is consistent with that proposed for other *fac*-$Re^I(CO)_3$ complexes supported by bipyridine ligands.[6] The size of the catalytic waves for both **8** and **12** are comparable, suggesting that both rhenium platforms catalyze the electrochemical reduction of CO_2 to similar extents (*vide infra*).

Upon confirming that both the rhenium platforms under consideration can activate CO_2, the photophysics and photocatalytic properties of these complexes were probed. Figure 3 presents the UV-vis absorption profiles of complexes **8** (red) and **12** (blue). The phenyl appended derivative (**8**) displays a UV-vis spectrum that is typical of that observed for *fac*-$Re^I(CO)_3$ complexes containing a bipyridine ligand with a strong absorption at 293 nm and an MLCT transition at 375 nm, which extends out past 425 nm. The BODIPY containing complex (**12**) displays similar bands along with a strong absorption ($\varepsilon \sim 60{,}000\ M^{-1}\cdot cm^{-1}$) centered at 525 nm consistent with excitation of the dipyrromethane moiety. As such, the existence of the BODIPY unit extends the ability of complex **12** to absorb light through the visible region out to nearly 600 nm.

In an effort to establish whether the appended phenyl or BODIPY moieties of **8** and **12** perturb the ability of these rhenium complexes to photochemically activate CO_2 a series of photolysis experiments were undertaken. Irradiation of a CO_2 saturated solution of complex **8** (1.5 mM) in DMF/ TEOA (5:1) with light of $\lambda_{ex} \geq 400$ nm resulted in the generation of CO as judged by gas chromatography. Quantification of the CO produced showed that this system operates with an initial TOF of approximately 5 hr^{-1} and an overall TON of 22 over the course of a 17 hour photolysis experiment. When the identical experiment was carried out using longer wavelength light ($\lambda_{ex} \geq 495$ nm), only trace levels of CO production were observed. This result is consistent with the low absorptivity of complex **8** at wavelengths longer than 430 nm. Similar results have been obtained using structurally simple rhenium tricarbonyl bipyridine complexes.[49]

The analogous experiments were also carried out for the BODIPY appended rhenium homologue (**12**). Irradiation of a 1.5 mM solution of **12** in CO_2 saturated DMF:TEOA (5:1) resulted in the formation of CO with an initial TOF of 4 hr^{-1} and a total TON of 20 over a 17 hour photolysis. Moreover, repeating this experiment using light of $\lambda_{ex} \geq 495$ nm only

led to the production of negligible levels of CO despite the ability of this complex to strongly absorb light in this region. When taken together, these results clearly show that the broader absorption profile of **12** is not manifest in an improved photocatalysis with CO_2 as compared to complex **8**.

In an effort to rationalize the similar activities of the two Re complexes described above, the photophysical properties of the BODIPY appended rhenium complex was probed in relation to a BODIPY photocontrol (**13**). The steady-state and time resolved emission properties of compound **13** were measured and are summarized in Table 1. This compound is highly emissive with a quantum yield of fluorescence of Φ_{Fl} = 86% and an excited state lifetime of τ_{Fl} = 4.87 ns. Both these values are typical of BODIPY derivatives derived from substituted pyrrole precursors.[39,46,50] Identical parameters were recorded for the BODIPY-appended Re complex (**12**). This compound also displays a high fluorescence quantum yield of Φ_{Fl} = 82% and an excited state lifetime (τ_{Fl} = 4.46 ns) that is only slightly shorter than that observed for the BODIPY control. These results indicate that electronic communication between the BODIPY moiety and Re center of **12** is poor and that the pendant dipyrromethane unit does not efficiently sensitize formation of the Re(bpy)$(CO)_3$Cl excited state or photoreduce the Re center.

The crystal structure of the bromide homologue of complex **8** provides a rationale for the poor coupling observed for the BODIPY appended Re complex. The molecular structure of this compound is presented in Figure 4 and crystal parameters are shown in Table S1. The conformation of this molecule is highly extended, which would place the BODIPY unit of **12** approximately 15.7 Å from the Re center of this complex. The long distance between the BODIPY moiety and metal center, coupled with the partially saturated linker would be expected to result in slow electron transfer or energy transfer kinetics.[51,52] As such, the lack of photocatalytic activity observed for **12** upon irradiation with $\lambda_{ex} \geq 495$ nm is likely a consequence of the molecular topology of the triazole containing bridge.

Additional evidence for the negligible electronic coupling between the BODIPY and Re centers is derived by comparison of the UV-vis profiles of **12** and **13**. As shown in Figure 3, the absorption profiles of the BODIPY moieties of these two compounds are virtually identical. Moreover, when the absorption profile of **12** is overlaid onto the composite spectrum of control compounds **8** and **13**, the two traces are nearly completely superimposable (Figure S1). When taken together, these spectra suggest that interaction between the BODIPY and rhenium centers of complex **12** is negligible in solution, which is consistent with the observed photophysics and catalysis.

Summary and Future Directions

The photochemical reduction of CO_2 to CO is a process of interest for the storage and distribution of solar energy. In this work, we have developed an assembly in which a BODIPY moiety was covalently tethered to a Re(bpy)$(CO)_3$Cl platform using a Huisgen coupling strategy. This complex (**12**) displays a rich redox chemistry as both the BODIPY and *fac*-$Re^{I}(CO)_3$ centers can be reduced by two electrons. Electrochemical experiments reveal that this BODIPY appended construct can store multiple electron equivalents and is capable of activating CO_2. Complementary photolysis experiments have demonstrated that this platform can drive the photochemical conversion of CO_2 to CO in a manner consistent with other Re(bpy)$(CO)_3$Cl complexes. Direct excitation of the *fac*-$Re^{I}(CO)_3$ center of compound **12** (λ_{ex} > 400 nm) is manifest in efficient conversion of CO_2 to CO, which is similar to the photocatalysis observed using a phenyl appended Re(bpy)$(CO)_3$Cl model complex (**8**).

While excitation of the rhenium center of **12** leads to photochemical reduction of CO_2 with modest TOF, the use of longer wavelength light does not drive the production of CO with high efficiency. While this finding is somewhat surprising given the strong absorptivity of this platform's BODIPY chromophore in the visible region, photophysical and structural interrogation of this and related complexes provide a rationale for this observation. A combination of UV-vis spectroscopy as well as steady state and time resolved emission measurements demonstrate that the electronic coupling between the BODIPY and *fac*-$Re^{I}(CO)_3$ centers of compound **12** are very poor. Structural analysis of a related phenyl appended assembly reveals that the triazole bridge of the systems studied places the BODIPY and Re moieties too far away from one another to permit efficient electronic communication between the two.

Although the lack of coupling precluded sensitization of the $Re(bpy)(CO)_3Cl$ center at longer wavelengths ($\lambda_{ex} \geq 495$ nm), this work provides several important realizations for development of improved photocatalysts that drive production of fuels from CO_2. One important finding is that the triazole moiety used to link the photocatalyst constituents does not interfere with the reductive photochemistry we have pursued. As such, Huisgen/click chemistry may provide a straightforward and versatile method for immobilization of $Re(bpy)(CO)_3Cl$ catalysts onto heterogeneous supports.[53] More importantly, the work reported herein clearly shows that BODIPY chromophores are tolerated under the standard photocatalysis conditions we have employed. This finding suggests that this versatile organic chromophore can be used in conjunction with *fac*-$Re^{I}(CO)_3$ complexes, and that properly designed assemblies in which coupling between the BODIPY and metal centers is optimized, may be promising platforms for the direct reduction of CO_2 using solar photons. In keeping with this realization, future work from our labs will explore the photophysical and photocatalytic properties of $Re(bpy)(CO)_3Cl$ derivatives supported by ligands in which BODIPY and/or other chromophores[28,54] are directly linked and strongly coupled to the bipyridine framework.

Supplementary Material

Refer to Web version on PubMed Central for supplementary material.

Acknowledgments

Research reported in this publication was supported by an Institutional Development Award (IDeA) from the National Institute of General Medical Sciences of the National Institutes of Health under grant number P20GM103541. GAA and JR were supported through an NSF sponsored LSAMP – "bridge to the doctorate fellowship" and a DuPont Young Professor award, respectively. JR also thanks the University of Delaware Research Foundation and the donors of the American Chemical Society's Petroleum Research Fund for financial support. DAL was sponsored by the Laboratory Directed Research and Development Program of Oak Ridge National Laboratory, managed by UT-Battelle, LLC, for the U. S. Department of Energy. NMR and other data were acquired at UD using instrumentation obtained with assistance from the NSF and NIH (NSF-MRI 0421224, NSF-CRIF CHE-0840401 and CHE-1048367, NIH P20 RR017716).

References

1. Olah GA, Goeppert A, Prakash GKS. J. Org. Chem. 2009; 74:487–498. [PubMed: 19063591]
2. Olah GA, Prakash GKS, Goeppert A. J. Am. Chem. Soc. 2011; 133:12881–12898. [PubMed: 21612273]
3. Rofer-DePoorter CK. Chem. Rev. 2012; 81:447–474.
4. Vennestrøm PNR, Osmundsen CM, Christensen CH, Taarning E. Angew. Chem. Int. Ed. 2011; 50:10502–10509.
5. Takeshita T, Yamaji K. Energy Policy. 2008; 36:2773–2784.

6. Kumar B, Llorente M, Froehlich J, Dang T, Sathrum A, Kubiak CP. Annu. Rev. Phys. Chem. 2012; 63:541–569. [PubMed: 22404587]
7. Smieja JM, Benson EE, Kumar B, Grice KA, Seu CS, Miller AJM, Mayer JM, Kubiak CP. Proc. Natl. Acad. Sci. USA. 2012; 109:15646–15650. [PubMed: 22652573]
8. Doherty MD, Grills DC, Muckerman JT, Polyansky DE, Fujita E. Coord. Chem. Rev. 2010; 254:2472–2482.
9. Morris AJ, Meyer GJ, Fujita E. Acc. Chem. Res. 2009; 42:1983–1994. [PubMed: 19928829]
10. Grodkowski J, Dhanasekaran T, Neta P, Hambright P, Brunschwig BS, Shinozaki K, Fujita E. J. Phys. Chem. A. 2000; 104:11332–11339.
11. Grodkowski J, Neta P, Fujita E, Mahammed A, Simkhovich L, Gross Z. J. Phys. Chem. A. 2002; 106:4772–4778.
12. Grodkowski J, Neta P. J. Phys. Chem. A. 2000; 104:1848–1853.
13. Grodkowski J, Behar D, Neta P, Hambright P. J. Phys. Chem. A. 1997; 101:248–254.
14. Behar D, Dhanasekaran T, Neta P, Hosten CM, Ejeh D, Hambright P, Fujita E. J. Phys. Chem. A. 1998; 102:2870–2877.
15. Craig CA, Spreer LO, Otvos JW, Calvin M. J. Phys. Chem. 1990; 94:7957–7960.
16. Sullivan BP, Meyer TJ. Organometallics. 1986; 5:1500–1502.
17. O'Toole TR, Sullivan BP, Bruce MRM, Margerum LD, Murray RW, Meyer TJ. J. Electroanal. Chem. Interfacial Electrochem. 1989; 259:217–239.
18. O'Toole TR, Margerum LD, Westmoreland TD, Vining WJ, Murray RW, Meyer TJ. Chem. Commun. 1985:1416–1417.
19. Agarwal J, Sanders BC, Fujita E, Schaefer IIIHF, Harrop TC, Muckerman JT. Chem. Commun. 2012; 48:6797–6799.
20. Agarwal J, Johnson RP, Li G. J. Phys. Chem. A. 2011; 115:2877–2881. [PubMed: 21410231]
21. Agarwal J, Fujita E, Schaefer HF, Muckerman JT. J. Am. Chem. Soc. 2012; 134:5180–5186. [PubMed: 22364649]
22. Sullivan BP, Meyer TJ. Organometallics. 1986; 5:1500–1502.
23. Sullivan BP, Meyer TJ. Chem. Commun. 1984:1244–1245.
24. Hori H, Johnson FPA, Koike K, Ishitani O, Ibusuki T. J. Photochem. Photobiol. A. 1996; 96:171–174.
25. Takeda H, Koike K, Inoue H, Ishitani O. J. Am. Chem. Soc. 2008; 130:2023–2031. [PubMed: 18205359]
26. Grills DC, Fujita E. J. Phys. Chem. Lett. 2010; 1:2709–2718.
27. Hawecker J, Lehn J-M, Ziessel R. Chem. Commun. 1984:328–330.
28. Pistner AJ, Yap GPA, Rosenthal J. J. Phys. Chem. C. 2012; 116:16918–16924.
29. Dubois KD, He H, Liu C, Vorushilov AS, Li G. J. Mol. Catal. A: Chem. 2012; 363–364:208–213.
30. Gholamkhass B, Mametsuka H, Koike K, Tanabe T, Furue M, Ishitani O. Inorg. Chem. 2005; 44:2326–2336. [PubMed: 15792468]
31. Tamaki Y, Watanabe K, Koike K, Inoue H, Morimoto T, Ishitani O. Faraday Discuss. 2012; 155:115–127. [PubMed: 22470970]
32. Gabrielsson A, Lindsay Smith JR, Perutz RN. Dalton Trans. 2008:4259–4269. [PubMed: 18682865]
33. Kiyosawa K, Shiraishi N, Shimada T, Masui D, Tachibana H, Takagi S, Ishitani O, Tryk DA, Inoue H. J. Phys. Chem. C. 2009; 113:11667–11673.
34. Schneider J, Vuong KQ, Calladine JA, Sun X-Z, Whitwood AC, George MW, Perutz RN. Inorg. Chem. 2011; 50:11877–11889. [PubMed: 22043811]
35. Windle CD, Câmpian MV, Duhme-Klair A-K, Gibson EA, Perutz RN, Schneider J. Chem. Commun. 2012; 48:8189–8191.
36. Jones G, Kumar S, Klueva O, Pacheco D. J. Phys. Chem. A. 2003; 107:8429–8434.
37. Pangborn AB, Giardello MA, Grubbs RH, Rosen RK, Timmers FJ. Organometallics. 1996; 15:1518.

38. Berg KE, Tran A, Raymond MK, Abrahamsson M, Wolny J, Redon S, Andersson M, Sun L, Styring S, Hammarström L, Toftlund H, Åkermark B. Eur. J. Inorg. Chem. 2001:1019–1029.
39. Nepomnyashchii AB, Pistner AJ, Bard AJ, Rosenthal J. J. Phys. Chem. C. 2013; 117:5599–5609.
40. Juris A, Balzani V, Barigelletti F, Campagna S, Belser P, Von Zelewsky A. Coord. Chem. Rev. 1988; 84:85.
41. Kawanishi Y, Kitamura N, Kim Y, Tazuke S. Riken Q. 1984; 78:212.
42. Calvert JM, Caspar JV, Binstead RA, Westmoreland TD, Meyer TJ. J. Am. Chem. Soc. 1982; 104:6620.
43. Sheldrick GM. Acta Cryst. 2008; A64:112–122.
44. Smeiga JM, Kubiak CP. Inorg. Chem. 2010; 49:9283–9289. [PubMed: 20845978]
45. Alvarez SG, Alvarez MT. Synthesis. 1997; 4:413–414.
46. Nepomnyashchii AB, Broring M, Ahrens J, Bard AJ. J. Am. Chem. Soc. 2011; 133:8633–8645. [PubMed: 21563824]
47. Rosenthal J, Nepomnyashchii AB, Kozhukh J, Bard AJ, Lippard SJ. J. Phys. Chem. C. 2011; 115:17993–18001.
48. Nepomnyashchii AB, Bard AJ. Acc. Chem. Res. 2012; 45(11):1844–1853. [PubMed: 22515199]
49. Hawecker J, Lehn JM, Ziessel R. Helv. Chim. Acta. 1986; 69:1990–2012.
50. Rosenthal J, Lippard SJ. J. Am. Chem. Soc. 2010; 132:5536–5537. [PubMed: 20355724]
51. Barbara PF, Meyer TJ, Ratner MA. J. Phys. Chem. 1996; 100:13148–13168.
52. Gietter AAS, Pupillo RC, Yap GPA, Beebe TP, Rosenthal J, Watson DA. Chem. Sci. 2013; 4:437–443.
53. Liu C, Dubois KD, Louis ME, Vorushilov AS, Li G. ACS Catal. 2013; 3:655–662.
54. Pistner AJ, Lutterman DA, Ghidiu MJ, Ma Y-Z, Rosenthal J. J. Am. Chem. Soc. 2013; 135:6601–6607. [PubMed: 23594346]

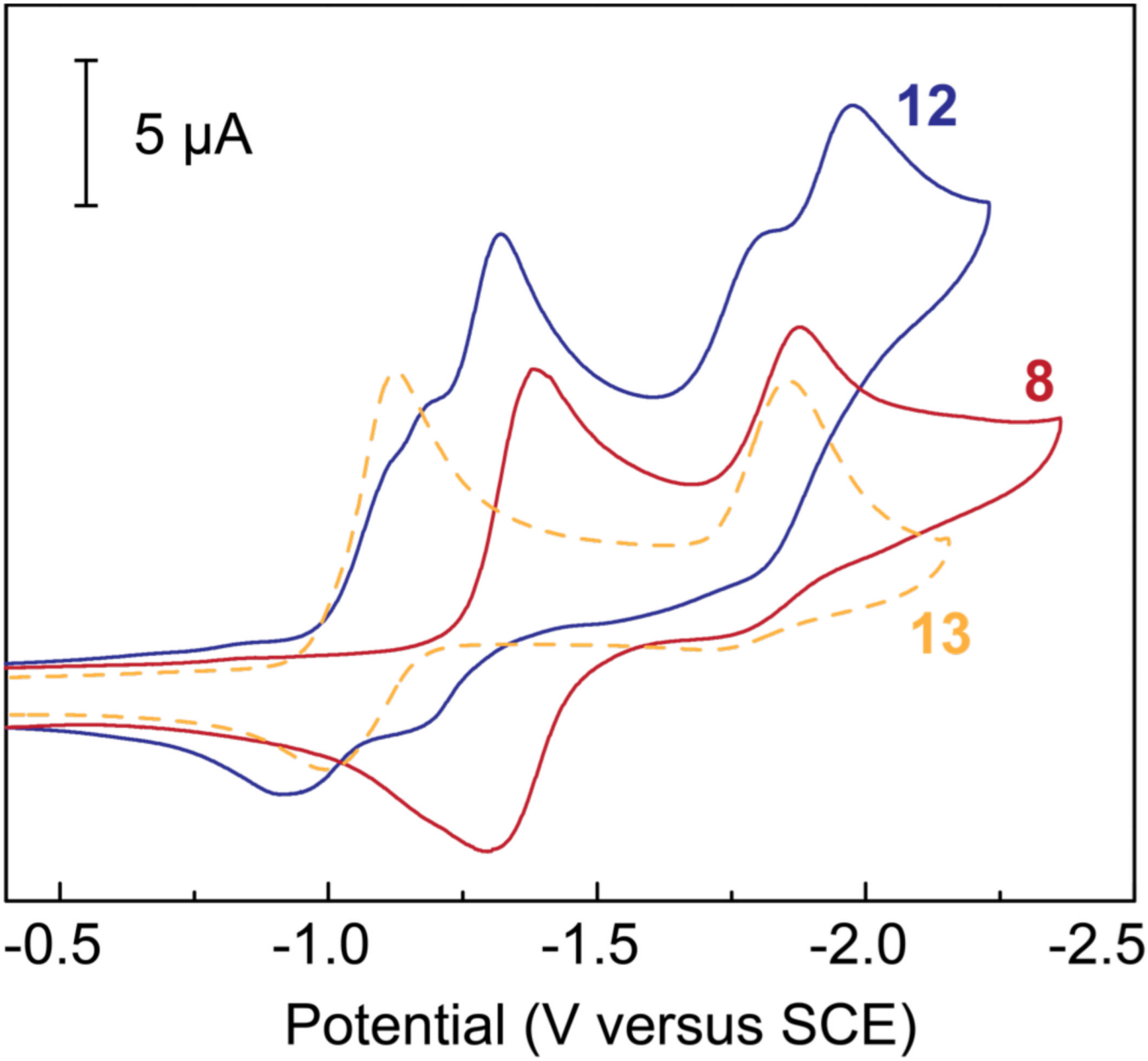

Figure 1.
Cyclic voltammograms recorded for 1.0 mM solutions of complex **8** (red), **12** (blue) and **13** (orange dashed) in DMF containing 0.1 M $TBAPF_6$ under an atmosphere of N_2. CVs were recorded using a glassy carbon working electrode and a Pt auxillary electrode at a scan rate of 100 mV/s.

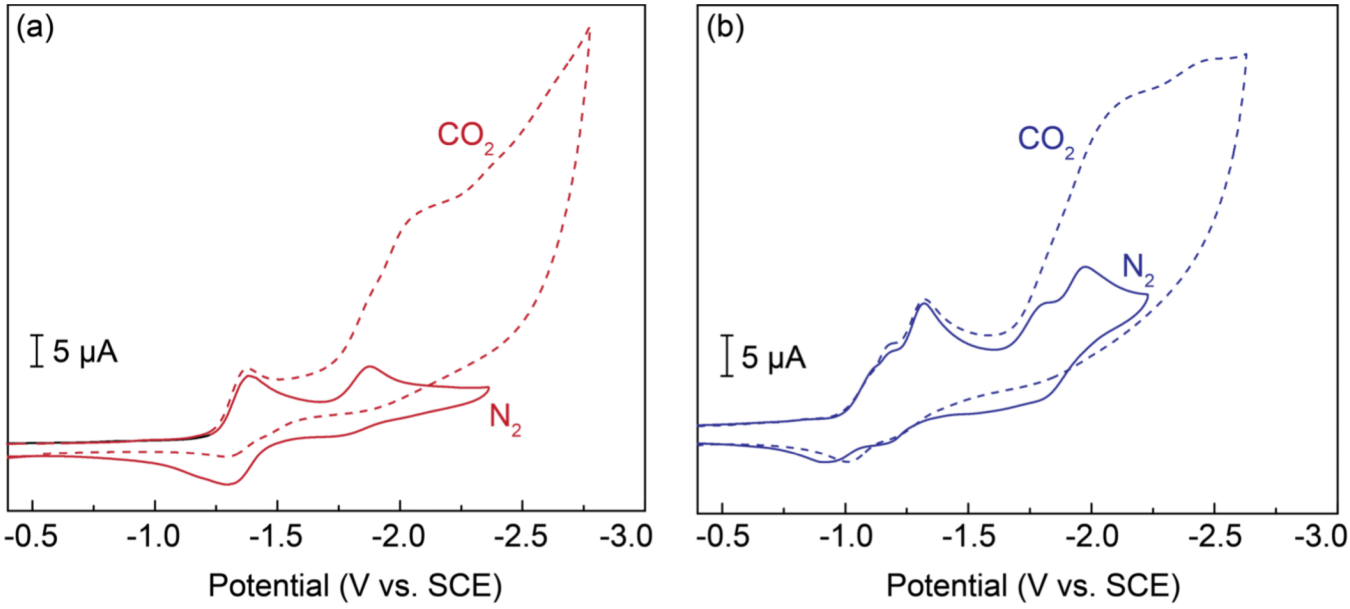

Figure 2.

Cyclic voltammograms recorded for 1.0 mM solutions of (a) complex **8** and (b) complex **12** in DMF containing 0.1 M $TBAPF_6$. Polarization curves were recorded under an atmosphere of either N_2 or CO_2. CVs were recorded using a glassy carbon working electrode and a platinum auxiliary electrode at a scan rate of 100 mV/s.

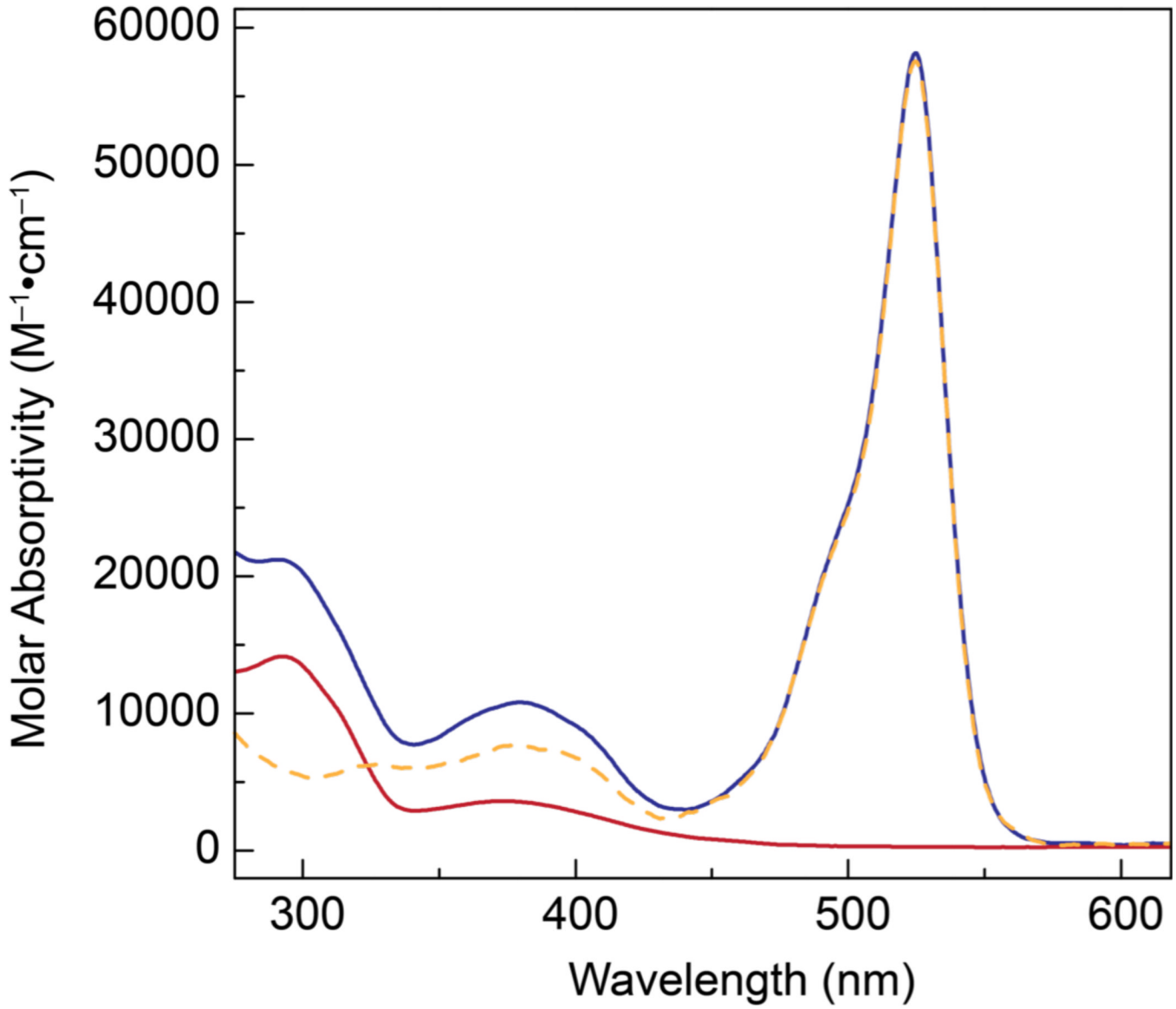

Figure 3.
UV-vis absorption profiles recorded for complex **8** (red), **12** (blue) and **13** (orange dashed) in DMF.

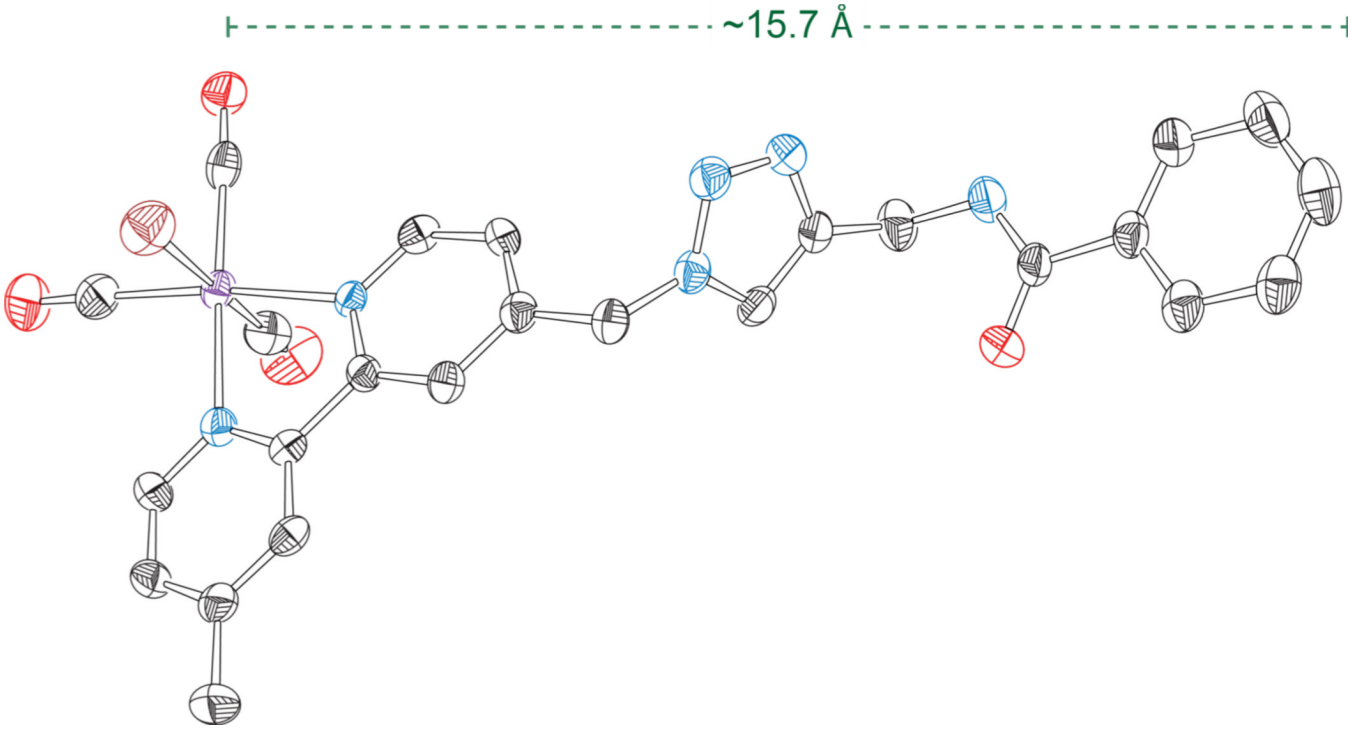

Figure 4.
Solid-state structure of the bromide homologue of compound **8**. Ellipsoids are shown at the 50% level and hydrogen atoms have been omitted for clarity.

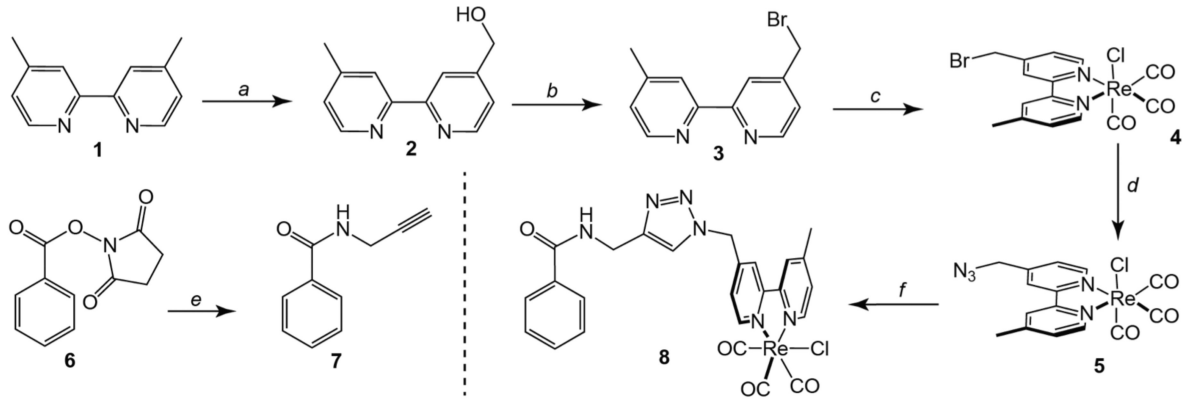

(a) 1. SeO_2, dioxane; 2. $NaBH_4$; (b) HBr, H_2SO_4; (c) $Re(CO)_5Cl$, toluene; (d) NaN_3, DMSO; (e) propargylamine, NEt_3; (f) **7**, $CuSO_4$, Ascorbic Acid, DMF

Scheme 1.
Synthesis of rhenium-phenyl control compound (8).

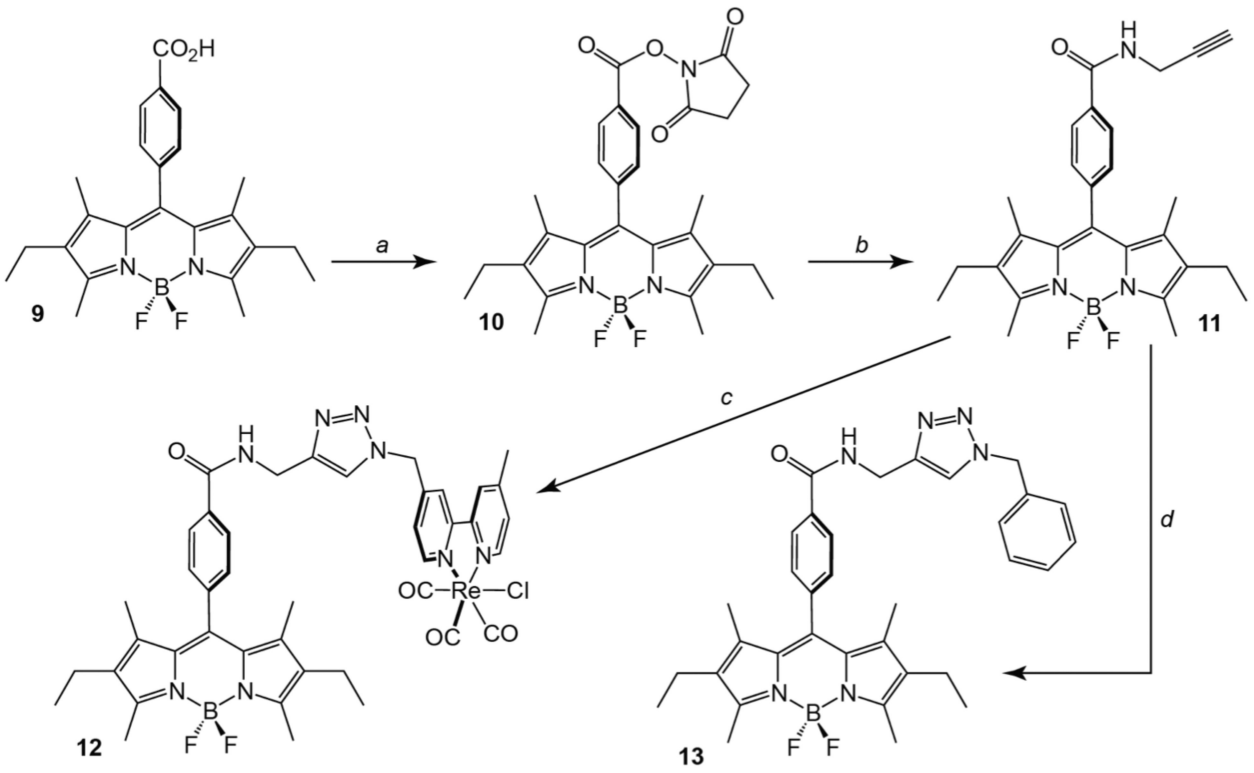

(a) NHS, EDC, DMF; (b) propargylamine, NEt_3; (c) **5**, $CuSO_4$, ascorbic acid, DMF; (d) **7**, benzylazide $CuSO_4$, ascorbic acid, DMF

Scheme 2.
Synthesis of BODIPY appended compounds 12 and 13.

Table 1

Overview of Photophysical and Photochemical Properties of Rhenium and BODIPY Constructs.

	Φ_{Fl}	τ_{Fl}	TOF	TON
8	——	——	5 hr^{-1}	22
12	82%	4.46 ns	4 hr^{-1}	20
13	86%	4.87 ns	——	——